Journal of Organometallic Chemistry 693 (2008) 2451–2457

Contents lists available at ScienceDirect

Journal of Organometallic Chemistry

journal homepage: www.elsevier.com/locate/jorganchem

Synthesis, spectroscopic properties and crystal structure of mononuclear tricarbonylrhenium(I) chloride complexes carrying 6-functionalised quinoxalines

Irene Veroni [a], Christiana A. Mitsopoulou [a,*], Fernando J. Lahoz [b]

[a] Inorganic Chemistry Laboratory, Department of Chemistry, National and Kapodistrian University of Athens, Panepistimiopolis, Zografou 15771, Greece
[b] Departamento de Quimica Inorganicas ICMA, Facultad de Ciencias, Universidad de Zaragozas CSIC, 50009 Zaragoza, Spain

ARTICLE INFO

Article history:
Received 3 April 2008
Received in revised form 24 April 2008
Accepted 24 April 2008
Available online 3 May 2008

Keywords:
2-(2′-Pyridyl)quinoxaline
Rhenium(I) carbonyl complexes
Crystal structure
6-functionalized pyridyl

ABSTRACT

Two quinoxaline derivatives pqCH$_3$ and pqCl (where pq stands for 2-(2′-pyridyl)quinoxaline) were prepared by condensation of 2-acetyl pyridyl with 2-amino-4-methylphenylamine or 2-amino-4-chlorophenylamine, correspondingly and were studied spectroscopically and electrochemically, in correlation with the originally reported pq. Their novel corresponded complexes namely, *fac*-[Re(CO)$_3$Cl(L)] (where L = pqCH$_3$ **2** and pqCl **3**) were synthesized, characterized, studied and compared to Re(CO)$_3$Clpq, **1**. Complex **2** crystallizes in space group *C*2/*c* with $a = 20.4476(17)$ Å, $b = 15.4521(13)$ Å, $c = 15.2887(13)$ Å, $\beta = 126.1210(11)^\circ$, $Z = 8$ and $V = 3902.0(6)$ Å^3. The substitution of –H by –CH$_3$ or –Cl at 6-position of pq has a minor electronic effect on the pyridyl ring of the ligands, but seems to influence the quinoxaline moiety enough to alter the spectroscopical and electrochemical features.

1. Introduction

Quinoxaline structure is recognized in a growing number of naturally occurring compounds such as riboflavin (vitamin B$_2$), flavoenzymes, molybdopterines and antibiotics of Streptomyces [1]. Quinoxaline derivatives have already been used as antibacterial, antiviral, anticancer, antifungal, antihelmintic and insecticidal agents [2]. The widely prescribed quinoxaline antibiotics are found to bind specifically by bisintercalation to double-stranded DNA [3] and to enhance peptide nucleic acid (PNA) binding to it [4], stimulating the research on the DNA-interactive ligands. In addition to this, some disubstituted quinoxaline derivatives have been found as potent antagonists of the quisqualate and kainate receptors on neurones of the central nervous system [5]. There has been a considerable amount of research into the biological effect of quinoxalines and could be supported by the use of carbonyl organometallic complexes; their diverse properties such as the IR spectra, the well-tailored photophysical behaviour and the varying degrees of resistance to decomposition by biological conditions anoint them as good candidates for biomarkers or for therapeutic purposes.

Herein we report on the synthesis, characterization and study of two novel quinoxaline ligands pqCH$_3$ and pqCl and their corresponding complexes to the *fac*-Re(CO)$_3$Cl organometallic core (Scheme 1). The above ligands are the 6-functionalised derivatives of 2-(2-pyridyl)-quinoxaline; the latter was produced via an unusual condensation reaction from 2-acetylopyridine and 1,2-diaminobenzene [6] and has been extensively studied because of its rich coordination chemistry in structural types and coordination modes [7]. The understanding of the structural and electronic properties of the quinoxaline derivatives is contributed by the study of their corresponding complexes Re(CO)$_3$Cl(pqCH$_3$), **2** and Re(CO)$_3$Cl(pqCl), **3** and the comparison to the prototype Re(CO)$_3$Cl(pq), **1** [8].

2. Experimental

2.1. Materials and equipment

Pq was synthesized following Hadjiliadis routine [6]. The starting materials 2-acetyl pyridyl, 2-aminophenylamine, 2-amino-4-methylphenylamine, 2-amino-4-chlorophenylamine and the catalyst for the organic syntheses methyl chloridocarbonate were obtained from Sigma–Aldrich Chemicals. The Re(CO)$_5$Cl was purchased from Alfa Aesar. The solvents used in UV-visible studies were purified to spectroscopic quality by standard methods [9]. The deuterated solvents, which were utilized in NMR experiments, were purchased from Aldrich and were of 99.99% purity.

FT-IR spectra in KBr pellets were recorded on a Nicolet Magna IR 560 spectrophotometer having 1.0 cm^{-1} resolution. Electronic absorption spectra were recorded on a Varian Cary 300 spectrometer, having a circulating thermostat. The solute concentration was $\approx 10^{-5}$ M and the samples were prepared just before the measurements. ^{1}H NMR measurements were performed using a Varian Unity Plus 300 NMR spectrometer. Samples were run in a 5 mm probe with deuterated solvents as internal lock and reference.

* Corresponding author. Tel.: +30 210 7274 452; fax: +30 210 8322 828.
E-mail address: cmitsop@chem.uoa.gr (C.A. Mitsopoulou).

0022-328X/$ - see front matter © 2008 Elsevier B.V. All rights reserved.
doi:10.1016/j.jorganchem.2008.04.035

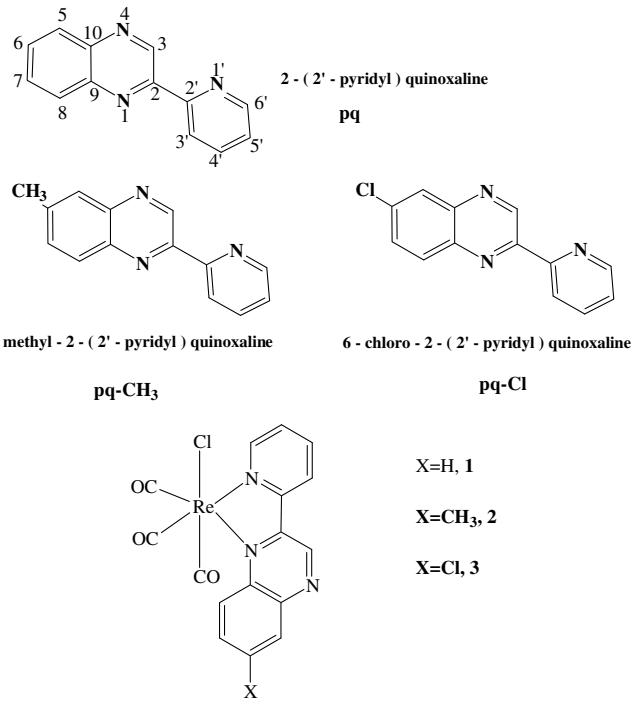

Scheme 1.

Microanalyses were performed with a Euro Vector EA 3000 analyzer. Cyclic voltammograms were recorded on an instrument of PINE Instrument Company using a type AFCBP1 potentiostat. Typically the samples were at 1 mM concentration in deaerated and dry DMF solvent with 0.1 M $(t\text{-But})_4NPF_6$ electrolyte. The scans were recorded at 100 mV s^{-1}.

2.2. Synthesis of ligands $pqCH_3$ and pqCl

2-Amino-4-functionalized-phenylamine (20.0 mmol) and methyl chloridocarbonate (0.4 mL, 5.20 mmol) were dissolved in 30 mL of iso-propanol in a round-bottom flask equipped with a magnetic stirrer and 2-acetylpyridine (4.5 mL, 40.1 mmol) was then added. The resulting solution was heated at 55 °C for 48 h and then cooled and kept at −5 °C for 8 h. The precipitate that appeared was filtered, washed with diethyl ether and dried under vacuum. Finally the crude solid was recrystallized from iso-propanol and the product was obtained as yellow needle crystals.

2.2.1. $pqCH_3$

Yield: 1.99 g (45%). Anal. Calc.: C, 76.0; H, 5.00; N, 18.99. Found: C, 76.04; H, 5.05; N, 18.97%.

2.2.2. pqCl

Yield: 1.45 g (30%). Anal. Calc.: C, 64.61; H, 3.34; N, 17.39. Found: C, 64.70; H, 3.40; N, 17.41%.

2.3. Synthesis of Re(I) complexes

The complexes were prepared by a substitution reaction between equimolar amounts of the diimine and $Re(CO)_5Cl$. The reactants were added in a Schlenk flask that contained methanol as solvent and refluxed under nitrogen atmosphere for 6 h. The resulting solution was filtered while hot to remove impurities. The filtrate was cooled until the desired crude complex precipitated and was isolated by filtration.

2.3.1. $Re(CO)_3Cl(pqCH_3)$, **2**

Complex **2** was recrystallized from a mixture of $CHCl_3$: tol = 4:1. Yield: 80%. Anal. Calc.: C, 38.8; H, 2.10; N, 7.97. Found: C, 38.2; H, 1.96; N, 8.03%.

2.3.2. $Re(CO)_3Cl(pqCl)$, **3**

Complex **3** was washed with CCl_4 and then recrystallized from $CHCl_3$. Yield: 78%. Anal. Calc.: C, 35.1; H, 1.47; N, 7.68. Found: C, 34.8; H, 1.45; N, 7.63%.

2.4. X-ray crystallography of **2**

Red lamina needles of **2**, suitable for X-ray structural determination, were grown by slow evaporation from a mixture of $CHCl_3$–toluene (3:1) at 279 K. A crystal with approximate dimensions 0.12 × 0.06 × 0.04 mm was secured to the end of a glass fibre with cyanocrylate glue. Crystallographic data are summarized in Table S1 as Supplementay material. Single-crystal X-ray diffraction experiments were carried out on a Bruker SMART APEX CCD diffractometer with graphite monochromated Mo Kα (λ = 0.71073 Å) radiation at 100 K. The semi-empirical method SADABS [10] was applied for absorption correction. The structure was solved by direct methods and refined by the full-matrix least-squares technique against F^2 with anisotropic temperature parameters for all non-hydrogen atoms. Data reduction and further calculations were performed using the SAINT [11], SHELXTL-97 [12] and MERCURY 1.4.1 program packages. Final least-squares refinement of 271 parameters resulted in residuals $R(F_o)$ of 0.0612 and $R'(F_o^2)$ of 0.0930.

3. Results and discussion

3.1. Preparation and NMR data

Quinoxaline derivatives were prepared in a one step reaction; 2-acetyl pyridyl reacts with 2-amino-4-methylphenylamine or 2-amino-4-chlorophenylamine to yield $pqCH_3$ or pqCl, correspondingly, as it is shown in Scheme 2. Apparently at first, a Schiff condensation takes place between the two amino groups of the diamine derivative and the carbonyls of two molecules of 2-acetyl pyridyl. The reaction intermediate undergoes an interesting cycloaddition, where a C–C bond between the two carbonyl carbons is formed while the one pyridine and the two $-CH_3$ groups become separated from the main aromatic frame. The procedure of the cyclo-addition is thermal and we postulate a radical driven reaction mechanism. The Re(I) complexes were prepared by substitution reactions between $Re(CO)_5Cl$ with equimolar amount of the ligand, as it is shown in Scheme 3. These reactions have high yield and produce minor sub-products that are easily removed.

In Table S2 (Supplementary material) are reported the proton chemical shifts of pqs in two solvents of different polarity. The

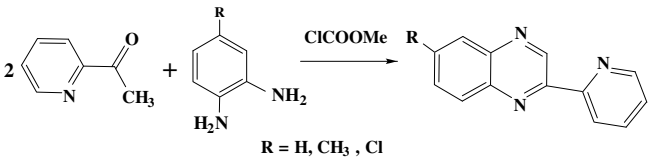

Scheme 2.

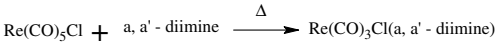

Scheme 3.

interpretation of the peaks to the corresponding protons was based on ^1H–^1H COSY experiments.

It has already been proven that pq is found in the *trans*-planar conformation in the solid phase [7]. The distinct nature and the extent of the interactions before and after the solvation of pqs define their configuration in solution. Indicative for the *anti*/*trans* configuration of pqs in solution were the NOESY ^1H–^1H NMR experiments of pqs in $CDCl_3$; the absence of cross-peaks in the spectra denotes the lack of proton interaction through space. In a potential *syn*/*cis* configuration, a cross-peak due to the interaction of $H_3 - H_{3'}$ should appear. In the following analysis we use as a starting point a *anti*/*trans* configuration of the organic molecule, considering that any deviation from it would normally come out in the course of the analysis.

The two most downfield peaks in the ^1H NMR spectra of pqs are attributed to H_3 and $H_{6'}$. This should be expected as they undergo the magnetic anisotropies of the near nitrogen atoms and the aromatic cloud of the rings. Among the two protons, H_3 is most downfield due to the electric field produced by the electric dipole of the adjacent pyridine group. The planarity of pqs should establish an inter-annular conjugation between its quinoxaline and pyridyl moiety that allows the π-deficient quinoxaline moiety to accept π electron density from the pyridyl ring; this is illustrated by the deshielding of $H_{3'}$, whose NMR signal follows that of $H_{6'}$.

The chemical proton shifts of the ligands are dependent on the solvents, moving towards lower field after an increase to the solvent polarity (Table S2). These variations differ for each proton and reflect at the same time the specific and the non-specific solute–solvent interactions. The general trend is disrupted at H_3 and $H_{3'}$; these protons shield more than the other protons of pq in polar solvents. Due to their position in the molecule, these two protons are the most influenced by their adjacent ring moiety. Any change in the relative position of the pyridine and the quinoxaline moiety in the molecule should directly be reflected on H_3 and $H_{3'}$'s behavior. The anomalous trend that the two protons exhibit as the solvent polarity changes can be taken as proof of an intramolecular structural change – a ring twisting, in particular. The twisting is the consequence of the effect that some solvents impose on the structure of the solute and the value of the twisting angle should depend on the solvent.

The comparison between the corresponding proton chemical shifts of the pqs points that the pyridyl moiety remains unaffected by the substitution at the position 6 of quinoxaline. On the contrary, the protons of the quinoxaline moiety at $pqCH_3$ are shielded in comparison to pq. In pqCl, the quinoxaline protons that are distant from –Cl are more deshielded in respect to pq, while H_5 and H_7 are shielded due to their proximity to –Cl.

The complexation of the pqs causes the removal of electron density to the $Re(CO)_3Cl$ core, which results in the deshielding of diimine protons. This is shown in Fig. S1(supplementary material), where the ^1H NMR spectra of pqs and their corresponding complexes are presented. The proton chemical shifts of **1**, **2** and **3** and their differences ($\Delta\delta$) from the corresponding substituted pqs are shown in Table 1. The largest proton shifts are recorded for $H_{3'}$ and then for $H_{8'}$; both of these are the closest to the metal. The proton chemical shifts at the pyridyl- part of the diimines remain almost unaffected by the different substitution at the quinoxaline part. Besides, the quinoxaline protons of **1** resonate at lower field than those of **2**, but only a little higher than the corresponding protons of **3**. As a whole, the differences $\Delta\delta$ are almost the same among the complexes. An interesting exception to the above is related with the $\Delta\delta$ of H_5; this is much higher in **1** than in the other complexes, which could imply that the substitution at 6-position hinders the electron transfer from N_4 to N_1 and then to the metal.

Table 1
^1H NMR proton chemical shifts of complexes (**1**)–(**3**) in d_6-DMSO and the chemical shift differences ($\Delta\delta$) between the protons of the complexes and the free ligands

	H_3	$H_{6'}$	$H_{3'}$	H_5	H_8	$H_{4'}$	H_6	H_7	$H_{5'}$	$-CH_3$
(**1**)	10.23	9.25	9.17	8.38	8.70	8.48	8.17	8.25	7.91	
$\Delta\delta$	0.44	0.46	0.69	0.21	0.59	0.44	0.28	0.38	0.35	
(**2**)	10.17	9.24	9.13	8.16	8.57	8.45	–	8.08	7.89	2.67
$\Delta\delta$	0.32	0.42	0.60	0.09	0.61	0.38	–	0.31	0.30	
(**3**)	10.25	9.26	9.18	8.35	8.66	8.50	–	8.31	7.93	
$\Delta\delta$	0.36	0.43	0.64	0.09	0.46	0.41	–	0.37	0.31	

3.2. Infrared data and absorption spectra

The IR spectra of the pqs are rather complicated but despite this, there are some features quite common to aromatic rings; in

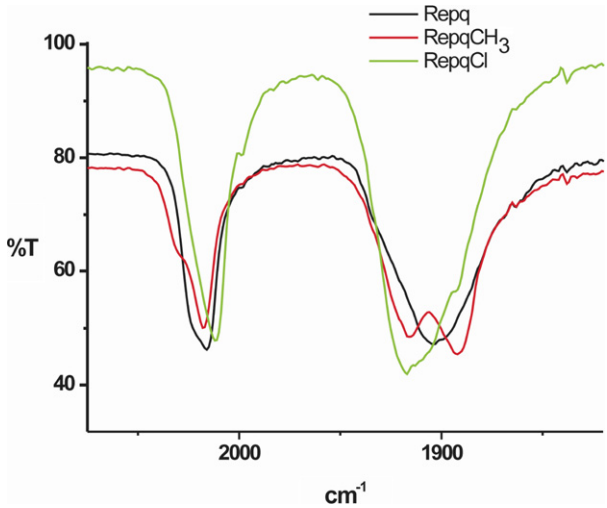

Fig. 1. CO stretching vibrational pattern in the IR spectra of the complexes **1**, **2** and **3** in KBr pellets.

Table 2
The CO IR stretching frequencies of the complexes in KBr pellets

Complex	A′(1)	E
1	2016	1903
2	2017	1916 (A″), 1892 (A′)
3	2011	1916

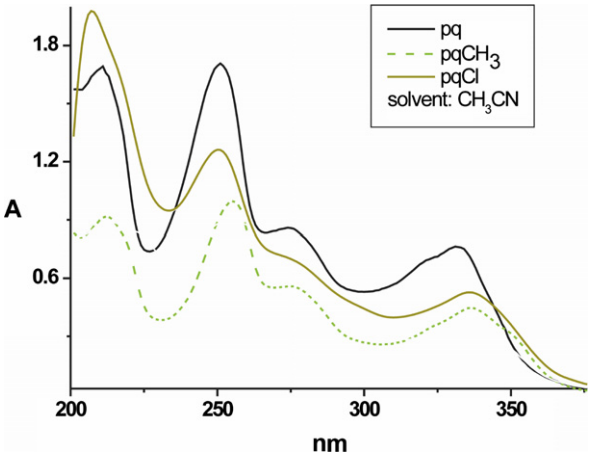

Fig. 2. UV–Vis absorption spectra of pq, $pqCH_3$ and pqCl in CH_3CN.

particular the bands at 3040, ~1580 and ~1060 cm^{-1} correspond to the stretches of C–H and C–C and the out of plane bending of C–H. The in- and out- of plane distortions of the 2-pyridyl ring of quinoxalines are quite characteristic and are found at 626 and 411 cm^{-1} [13].

IR spectra recorded in KBr pellets displayed three metal carbonyl bands in the region of 2023–1890 cm^{-1}, as is seen in Fig. 1. This is consistent with pseudo-C_{3v} symmetry for the compounds with a α_1 band and an *e* band split by the lowering in symmetry to α'' and α'. Under the conditions of the measurement, the latter bands are clearly separated only in **2**. The wavenumbers of the CO stretches are very sensitive to the d_p electron density (oxidation state) of the rhenium center. The constancy of the wave numbers among the complexes, as is seen in Table 2, indicates that the ligands induce an equivalent perturbation on the metal centre.

The electronic absorption spectra of quinoxalines have many similarities, as it is seen in Fig. 2. They contain four main bands and many shoulders between ~200 and ~350 nm; the corresponding wavelength maxima are included in Table 3. The absorption spectra of the 2-pyridyl quinoxalines are quite similar to the well-studied spectrum of quinoxaline [14] apart from the band at ~275 nm and two shoulders on the band of the ~330 nm, which are absent from the spectrum of quinoxaline. The above features could be attributed to transitions that are centered on the pyridyl moiety. In addition to this, the bands of quinoxaline are ~15 nm at lower wavelengths in comparison to its pyridyl derivatives, something quite expected due to the enhanced delocalization of the π-electron density on the pyridyl ring.

The λ_{max} of the lowest energy bands of $pqCH_3$ and pqCl are red-shifted by ~5 nm in respect to pq, while small differences in position and intensity are also observed at the second highest energy band at ~253 nm. The molar absorption coefficient of the latter band has been estimated to be 1.7 times lower for pqCl in respect to the other two quinoxalines as a result of the heavy atom effect.

The change of the solvents has only a minor effect on the shape and position of the bands of the free ligands, as is observed in Table 3. This could be a consequence to the small change of electron charge during an electronic transition.

Electronic absorption spectra of the complexes in various solvents are indicated in Fig. 3 and the corresponding data are included in Table 4. As a whole, the spectra consist of two main bands; a broad low-energy band and a narrower, more intense, high-energy band at the UV region. The UV bands resemble in shape and position the lowest-energy ones in the corresponding spectra of the free diimines, despite they are found at higher wavelengths and are more structured. Their structure consists of two peaks that are more easily observed in polar solvents. The change of the solvent mainly affects the position of the low-energy band that exhibits negative solvatochromism – thus, it blue-shifts as the polarity of the solvent increases. According to the theory of dielectric polarization, negative solvatochromism is expected for transitions from a ground state with a high dipole moment to an excited state with a smaller one, so that the (di)polar solvents stabilize the GS more than the ES, leading to an increased transition energy [15].

The shape along with the position and the solvent dependence of the low-energy band denote its (Re)$d\pi \rightarrow \pi^*(L)$ charge-transfer (MLCT) character, which agrees with previous interpretations of

Table 4
The wavelength maxima of the absorption bands of **1**, **2** and **3** in two solvents and the wavelength difference of their lowest-energy band between these solvents

Solvent	(**1**)	(**2**)	(**3**)
$CHCl_3$	**458**, 371, 352	**450**, 378, 358	**468**, 377, 360
Dmf	**431**, 371, 355	**423**, 375, 360	**437**, 377, 362
$\Delta\lambda_{LE}$	27	27	31

Table 3
λ_{max} (nm) of the absorption spectra of pq, $pqCH_3$ and pqCl in three different solvents (sh stands for shoulder)

Solvent	pq	$pqCH_3$	pqCl
MeOH	211, 250, 275, 322sh, 333, 353sh, 357sh	212, 255, 277, 337, 351sh, 357sh	212, 249, 251, 274sh, 338, 349sh, 353sh, 358sh
CH_3CN	211, 251, 275, 322sh, 332	212, 254, 276, 327sh, 337, 348sh, 353sh	207, 250, 274, 325sh, 336, 350sh, 353sh, 356sh
CCl_4	276, 323sh, 329sh, 334, 345sh, 348sh	278, 285sh, 326sh, 337, 350sh, 355sh	256sh, 282sh, 327sh, 339, 350sh, 353sh

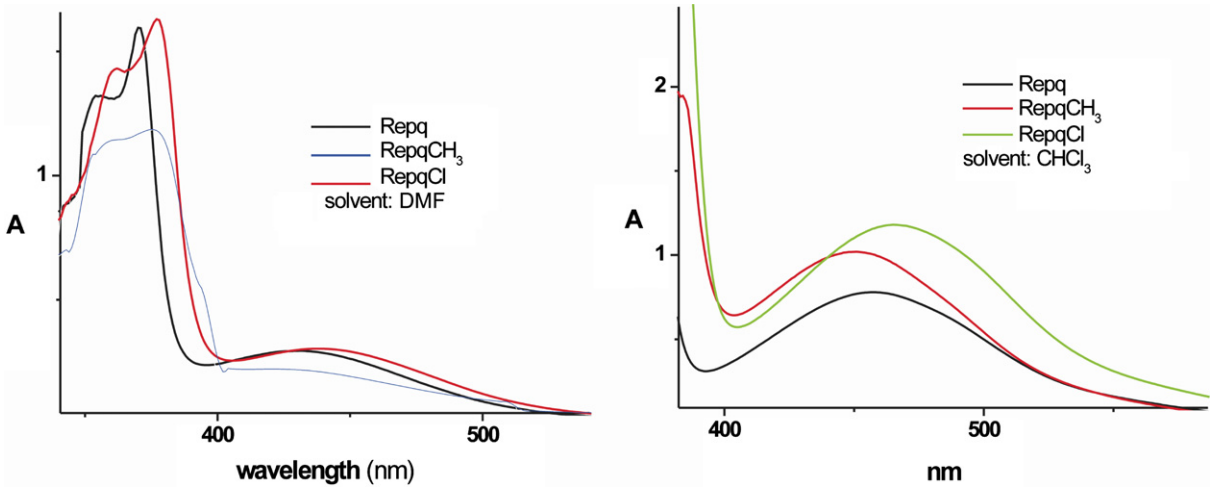

Fig. 3. UV–Vis absorption spectra of the complexes **1**, **2** and **3** in two different solvents.

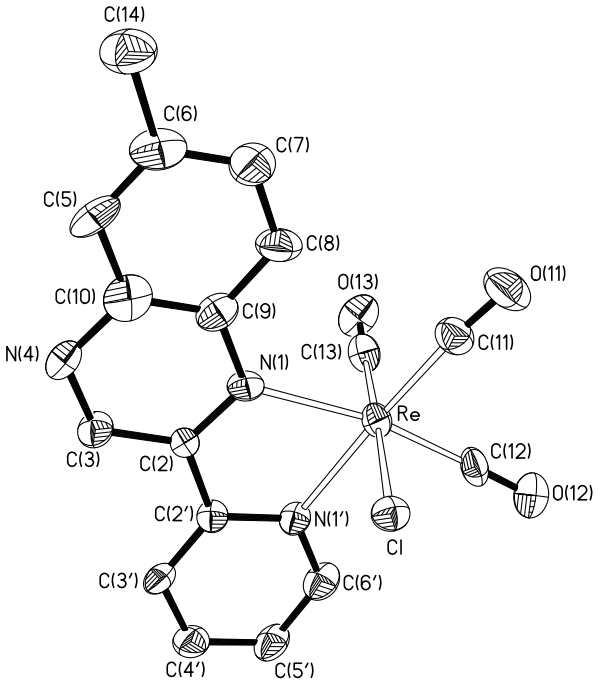

Fig. 4. An ORTEP drawing of complex **2** with the atomic numbering scheme.

many mononuclear metal tricarbonyl Re complexes [16]. The resemblance of the high-energy structured band with the band of the free ligands implies its IL π(diimine) → π^*(diimine) character, though we should not ignore the potential involvement of Re → CO MLCT transitions.

The comparison of the MLCT band maxima of **1**, **2** and **3** shows that the $-CH_3$ due to its electron donating effect, increases the π^* diimine energy level, which enhances the MLCT $d\pi \rightarrow \pi^*$ transition energy about 8 nm. On the other hand, the electron drawing –Cl group has the opposite effect and lowers the MLCT $d\pi \rightarrow \pi^*$ transition energy about 10 nm. The substitution of –H by $-CH_3$ and –Cl groups in **2** and **3** lowers the energy of IL π(diimine) → π^*(diimine) transitions in the complexes as it is indicated in Fig. 4. Finally, the three complexes exhibit similar solvatochromic behaviour; despite **3** seems to be slightly more solvatochromic than the others.

3.3. Crystal structure of *2*

The structure of complex **2** was determined by single-crystal X-ray diffraction methods. A suitable crystal of **2** was obtained by recrystallization from $CHCl_3$/toluene solution. Actually, most of the crystals obtained showed a twinned nature. Eventually data were collected on a small – apparently single – crystal that upon diffraction shows a minor twinned component (less than 5–10% approx.). Moreover, several residual peaks indicated the presence of disordered solvent in the crystal structure. A planar six-membered ring was clearly identified around a center of symmetry (only three independent C atoms). The existence of a second disordered molecule was supported by the presence of additional residuals in the solvent region, together with the refinement of very high anisotropic thermal parameters for these three atoms. The aforementioned two facts contribute to increase the value of R factor over current standard values, although no indication of errors in the structure determination are detected.

Table 5
Selected molecular parameters (distances in Å, angles in °) of compound **2**

Bond distances (Å)			Bond angles (°)	
Re	C_{12}	1.912(10)	Cl–Re–C_{13}	177.94(3)
	C_{13}	1.912(10)	N_1–Re–C_{12}	169.32(3)
	C_{11}	1.929(10)	$N_{1'}$–Re–C_{11}	173.95(4)
	$N_{1'}$	2.175(7)	$N_{1'}$–Re–N_1	74.80(3)
	N_1	2.230(7)		
	Cl	2.464(2)		
O_{11}	C_{11}	1.146(11)		
O_{12}	C_{12}	1.150(11)		
O_{13}	C_{13}	1.143(11)		
$C_{2'}$	C_2	1.462(11)		

An ORTEP drawing of **2** is shown in Fig. 4 and selected bond distances and angles are given in Table 5. The numbering of the atoms in Fig. 4, Table 5 and in the corresponding discussion of the complex that follows, is different from the one kept for the ligand pq, but still in accordance with IUPAC rules for complexes.

The structure is based on mononuclear units with eight molecules of the complex in the unit cell. The molecule has $\mathbf{C}_1$ symmetry. The coordination geometry at the Re atom is distorted octahedral with three carbonyl ligands arranged in a facial fashion. The $N_{1'}$—Re—N_1 angle is 74.8 (3)° and is significantly smaller than 90°; this results from the small bite angle of the diimine. The latter has already referred to [8]. Actually, this angle is 73.7(1)° and 75.27(14)° for the complexes $Re(CO)_3$Cldpq, (dpq = 2,3-di(2-pyridyl)quinoxaline) [8] and $Re(CO)_3$Clppb, (ppb = [2,3-α:3′,2′-c]dipyridophenazine) [8], respectively, implying that the 2-position of a substituent on pq has a significant role on the structural and electronic properties of these complexes. The rhenium–carbonyl bond lengths do not show any significant differences [1.912(11), 1.912(10) and 1.143(10) Å] but are consistent with those observed in similar complexes [8,17]. The Re—N_1' bond (2.175(7) Å) is rather smaller than the Re–N_1 bond (2.230(7) Å), but both are in the range expected for such complexes. Again, these bond distances are between those of the complexes $Re(CO)_3$Cldpq and $Re(CO)_3$Clppb. The bond of the metal to the quinoxaline moiety of the diimine is longer probably due to its steric effect. The axial level of the complex contains the Cl, Re, C_{13} and O_{13} atoms, without any declinations. The equatorial level contains the carbons of $pqCH_3$ and the two carbonyls; only O_{11} declines, as it is 0.399 Å out of it. The two levels form an 84.5° angle, instead of the 90° angle expected in an octahedral symmetry. Besides, the section of the two levels forms a ~16° angle with the line that bisects the bite angle N_1–Re–N_1. Thus, the usual planar arrangement of metal centre, diimine ligand and equatorial CO's is not observed due to the steric strain between the hydrogen atoms of the outer aromatic ring and the equatorial carbonyl ligand (Fig. 4). These distortions are less pronounced than those which have been referred to for the complexes $Re(CO)_3$Cldpq and $Re(CO)_3$Clppb [8]. This means that there are no potentially destabilizing interactions between the pyridyl ring of **2**, whereas the existence of a substituent at the 2-position of the quinoxaline ring increases the steric interactions between the pyridyl rings.

The significance of these distortions and variations observed between different complexes are yet to be explained and is currently underway in our lab.

3.4. Redox data

The electrochemistry of the ligands was investigated using cyclic voltammetry; the electrochemical data are included in the Table 6 and typical cyclic voltammograms of pq–Cl is presented in Fig. 5. Pq displays two non-irreversible couples that correspond to a well-resolved reduction wave approximately at –1.27 V and a less resolved one at more positive potentials. The CVs of the 6-functionalized pq derivatives are obviously more complicated (Fig. 5), as they include more cathodic waves. The free ligands display shifts in their reduction potential commensurate with the electron

Table 6
Electrochemical data for the reduction of pqs by cyclic voltammetry using carbon electrode in DMF solution containing 0.1 M NBu_4PF_6

	$E_{p(c)}$ (V)	$E_{p(a)}$ (V)
Pq	−1.33, −0.71	−1.20, +0.03
$PqCH_3$	−1.38, −1.24, −1.07	−1.25, −0.5
PqCl	−1.19, −1.05, −0.93, −0.59	−1.09, −0.38

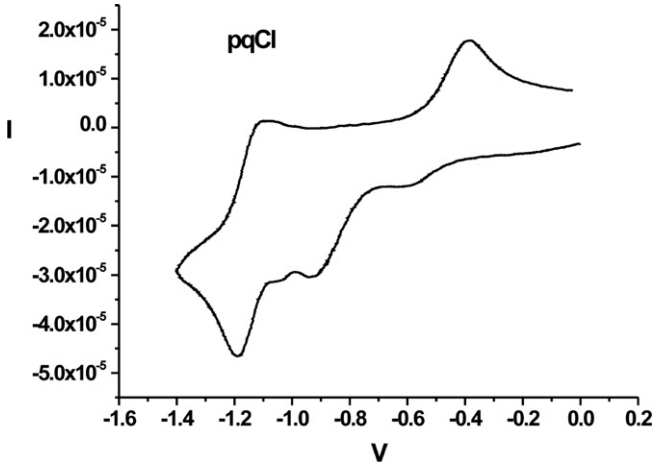

Fig. 5. CV of pq–Cl.

donating or withdrawing character of the substituent, considering that the reduction of the pqX results in the formation of anion-radicals. The presence of electro-withdrawing groups facilitates the reduction and lowers the reduction potential, as it stabilizes the anion-radicals. On the other hand, the basic cathodic bands are almost at the same position for the three ligands, which could mean either that the reduction is oriented on the pyridyl moiety or that a dissociation of the substituent group precedes. The latter has been reported in a series of chlorinated quinoxalines, where an electrochemical cleavage of the bond C–Cl takes place and a common anion-radical is formed and commonly reduced [18]. In our case, the two electrochemical waves before reduction at ~−1.43 to −1.33 V could involve bond cleavages.

The electrochemical data of **1**, **2** and **3** and a typical cyclic voltammogram of **3** are indicated in Table 7 and Fig. 6, respectively. The CVs reveal two reduction waves in a lower potential than the free ligands. The first electrochemical wave is reversible and can be attributed to the one electron reduction of the complexed pqX, as it is shown by the following equation:

$$(pqX)Re(CO)_3Cl + e^- \rightarrow (pqX^-)Re(CO)_3Cl \quad (1)$$

The corresponding reduction potentials are quite low in respect to others of similar complexes [19] and follow the order $E_{1/2(\mathbf{3})} < E_{1/2(\mathbf{1})} < E_{1/2(\mathbf{2})}$, which coincides with the π^* energy level of the ligands.

The second reduction of the complexes is irreversible and takes place at higher potentials than the first one. It could possibly involve either the reduction of the metal center Re(I) → (0) or a second reduction of the diimines $pqX^-/^{2-}$. The second scenario seems

Table 7
$E_{1/2}$ (V) of the two reduction waves of complexes **1**, **2** and **3** by cyclic voltammetry, using carbon electrode in DMF solution containing 0.1 M NBu_4PF_6

Complex	$E_{1/2(\mathbf{1})}$ (V)	$E_{1/2(\mathbf{2})}$ (V)
1	− 0.52	− 0.70
2	− 0.54	− 0.72
3	− 0.44	− 0.61

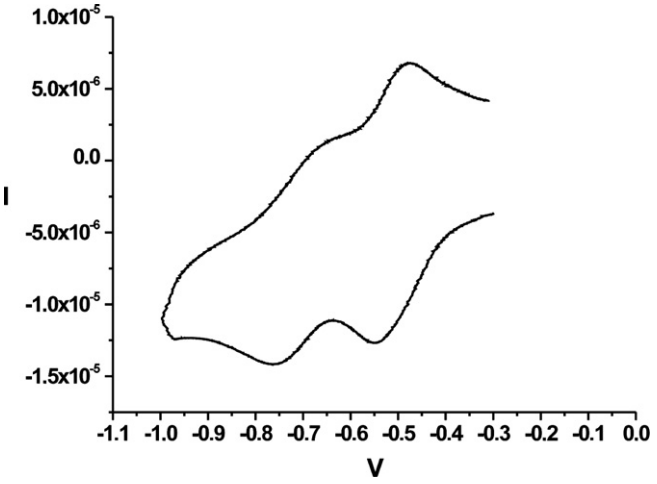

Fig. 6. CV of $Re(CO)_3Cl(pq–Cl)$.

more adequate for our case as the second reduction potential changes along the complexes, in a similar way to the first reduction potential. An interesting observation is that the difference between the second and the first reduction potential is quite the same for the three complexes, which could support the hypothesis that the second electron of reduction is oriented on the pyridyl moiety of the ligands.

4. Conclusion

Two new 6-substituted derivatives of pq have been synthesized and characterized along with the un-substituted pq. The electroctrochemical and electronic absorption properties of these ligands are consistent with the electron withdrawing and donating effects of the substituents. All three ligands have been coordinated to the $Re(CO)_3Cl$ core. The electronic properties of the resulting complexes also mirror the electron driving effects of the substituents, indicating that the former can be well tuned by altering the substituent at the 6-position of the pq.

Electrochemical studies reveal that not only the first reversible reduction of the $Re(CO)_3Cl$-complexes but also the second one is based on the quinoxaline moiety.

The elucidation of the crystal structure of **2** and its comparison with similar complexes reveal that the substitution of –H at 6-position of pq has a minor effect on its molecular structure retaining the planarity of the quinoxaline ligand. The latter is very important since complexes carrying these ligands could used as intercalators to DNA indicating therapeutic properties [20] or even as photoprobes or photooxidising agents of DNA, since they are powerful oxidizing agents and their photochemical and electrochemical properties can well be tuned.

Acknowledgement

We would like to thank the Special Research Account of University of Athens for partial financial support.

Appendix A. Supplementary material

CCDC 683203 contains the supplementary crystallographic data for $C_{20}H_{15}N_3O_3Re$. These data can be obtained free of charge via http://www.ccdc.cam.ac.uk/conts/retrieving.html, or from the Cambridge Crystallographic Data Centre, 12 Union Road, Cambridge CB2 1EZ, Uk; fax:(+44) 1223-336-033; or e-mail: deposit@ccdc.cam.ac.uk. Crystallographic data are also included in Table

S1; whereas Table S2 and Figure S1 provide the NMR data and spectra for the pq ligands. Supplementary data associated with this article can be found, in the online version, at doi:10.1016/j.jorganchem.2008.04.035.

References

[1] (a) M.M. Ali, M.M.F. Ismail, M.S.A. EI-Gabby, M.A. Zahran, T.A. Ammar, Molecules 5 (2000) 864;
(b) M.G. Knize, C.P. Salmon, E.C. Hopmans, J. Chromatogr., A 763 (1997) 179;
(c) F.F. Seelig, Z. Naturforsch., A 34 (1979) 986;
(d) H.-R. Park, T.H. Kim, K.-M. Bark, Eur. J. Med. Chem. (2002) 1;
(e) G. Sakata, K. Makino, Y. Kurasawa, Heterocycles 27 (1998) 2481.

[2] (a) B. Zarranz, A. Jaso, I. Aldana, A. Monge, Bioorg. Med. Chem. 12 (2004) 3711;
(b) Y.B. Kim, Y.H. Kim, J.Y. Park, S.K. Kim, Bioorg. Med. Chem. Lett. 14 (2004) 541;
(c) S.T. Hazeldine, L. Polin, J. Kushner, K. White, T.H. Corbett, J. Biehl, J.P. Horwitz, Bioorg. Med. Chem. 13 (2005) 1069.

[3] K.J. Addess, J.S. Sinsheimer, J. Feigon, Biochemistry 32 (1993) 2498.

[4] N.E. Mollegaard, C. Bailly, M.J. Waring, P.E. Nielsen, Biochemistry 39 (2000) 9502.

[5] H. Lavreysen, T. Willemoens, J.E. Leysen, A.S.J. Lesage, Europ. J. Neurosci. 21 (2005) 1610.

[6] S. Kasselouri, A. Garoufis, A. Katehanakis, G. Kalkanis, S.P. Perlepes, N. Hadjiliadis, Inorg. Chim. Acta 207 (1993) 255.

[7] (a) I. Veroni, A. Rontoyianni, C.A. Mitsopoulou, Dalton Trans. (2003) 255;
(b) I. Veroni, C. Makedonas, A. Rontoyianni, C.A. Mitsopoulou, J. Organomet. Chem. 691 (2006) 267;
(c) I. Veroni, C.A. Mitsopoulou, F.J. Lahoz, J. Organomet. Chem. 691 (2006) 5955;
(d) C. Makedonas, I. Veroni, C.A. Mitsopoulou, Eur. J. Inorg. Chem. (2007) 120;
(e) J.C. Plakatouras, N. Hadjiliadis, S.P. Perlepes, A. Albinati, G. Kalkanis, Polyhedron 12 (1993) 2069;
(f) E.G. Bakalbassis, J. Mrozinski, S.P. Perlepes, N. Hadjiliadis, F. Lianza, A. Albinati, Polyhedron 13 (1994) 3209;
(g) S. Kasselouri, A. Garoufis, S. Paschalidou, S.P. Perlepes, I.S. Butler, N. Hadjiliadis, Inorg. Chim. Acta 227 (1994) 129;
(h) A. Garoufis, A. Koutsodimou, C.P. Raptopoulou, A. Simopoulos, N. Katsaros, Polyhedron 18 (1999) 3005.

[8] (a) M.R. Waterland, T.J. Simpson, K.C. Gordon, A.K. Burrell, Dalton Trans. (1998) 185;
(b) M.I.J. Polson, S.L. Howell, A.H. Flood, A.G. Blackman, K.C. Gordon, Polyhedron 23 (2004) 1427.

[9] D.D. Perrin, W.L.F. Armarego, Purification of Laboratory Chemicals, 3rd ed., Pergamon Press, 1988.

[10] G.M. Sheldrick, SADABS, Bruker AXS Inc., Madison, WI, 1997.

[11] SAINT V5.00, Area Detector Control and Integration Software, Bruker AXS Inc., Madison, WI, 1998.

[12] G.M. Sheldrick, SHELXTL-97 V5.10, Bruker AXS Inc., Madison, WI, 1997.

[13] A.S. Kumbhar, N.R. Dhumal, S.P. Gejji, J. Mol. Struct. (Theochem) 589 (2002) 301.

[14] R. Czerwieniec, J. Herbich, A. Kapturkiewicz, J. Nowacki, Chem. Phys. Lett. 325 (2000) 589.

[15] C.J.F. Böttcher, Theory of Electric Polarization, vol. 1, Elsevier, Amsterdam, 1973.

[16] D.J. Stufkens, A. Vlček Jr., Coord. Chem. Rev. 177 (1998) 127.

[17] (a) E.W. Abel, V.S. Dimitrov, N.J. Long, K.G. Orrell, A.G. Osborne, H.M. Pain, V. Sik, M.B. Hursthouse, M.A. Mazid, J. Chem. Soc., Dalton Trans. (1993) 597;
(b) D.A. Bardwell, F. Barigelletti, R.L. Cleary, L. Flamigni, M. Guardigli, J.C. Jeffery, M.D. Ward, Inorg. Chem. 34 (1995) 2438;
(c) P. Chen, M. Curry, T.J. Meyer, Inorg. Chem. 28 (1989) 2271;
(d) L.E. Helberg, J. Barrera, M. Sabat, W.D. Harman, Inorg. Chem. 34 (1995) 2033;
(e) N.M. Iha, G.J. Ferraudi, J. Chem. Soc., Dalton Trans. (1994) 2565;
(f) R.J. Shaver, M.W. Perkovic, D.P. Rillema, W. Clifton, Inorg. Chem. 34 (1995) 5446;
(g) V.W.-W. Yam, V.C.-Y Lau, J.K.-K. Cheung, Chem. Soc., Chem. Commun. (1995) 259;
(h) V.W.-W. Yam, K.M.-C. Wong, V.W.-M. Lee, K.K.-W. Lo, K.-K. Cheung, Organometallics 14 (1995) 4034.

[18] (a) R. Sahai, D.P. Rillema, R. Shaver, S. Van Wallendael, D.C. Jackman, M. Boldaji, Inorg. Chem. 28 (1989) 1022;
(b) S. Van Wallendael, R.J. Shaver, D.P. Rillema, B.J. Yoblinski, M. Stathis, T.F. Guard, Inorg. Chem. 29 (1990) 1761.

[19] M.S. Mubarak, D. G Peter, J. Electroanal. Chem 507 (2001) 110.

[20] (a) C. A Mitsopoulou, C.E. Dagas, C. Makedonas, J. Inorg. Biochem. 102 (2008) 77;
(b) C. A Mitsopoulou, C.E. Dagas, C. Makedonas, Inorg. Chim. Acta 361 (2008) 1973.